INTERNATIONAL JOURNAL FOR NUMERICAL METHODS IN ENGINEERING
Int. J. Numer. Meth. Engng 2014; **00**:1–24
Published online in Wiley InterScience (www.interscience.wiley.com). DOI: 10.1002/nme

Discrete Lagrangian Mechanics for Nonseparable Nonsmooth Systems †

DAVID PEKAREK* and TODD D. MURPHEY

SUMMARY

We consider event-driven schemes for the simulation of nonseparable mechanical systems subject to holonomic unilateral constraints. Systems are modeled in discrete time using variational integrator (VI) theory, by which equations of motion follow from discrete variational principles. For smooth dynamics, VIs are known to exactly conserve a discrete symplectic form and a modified Hamiltonian function. The latter of these conservation laws can play a pivotal role in stabilizing the energy behavior of collision simulations. Previous efforts to leverage modified Hamiltonian conservation have been limited to integrators using the Störmer-Verlet method on separable, nonsmooth Hamiltonian mechanical systems. We generalize the existing approach to the family of all VIs applied to nonseparable, potentially nonconservative Lagrangian mechanical systems. We examine the properties of the resulting integrators relative to other structured collision simulation methods in terms of conserved quantities, trajectory errors as a function of initial condition, and required computation time. Interestingly, we find that the modified collision Verlet algorithm (MCVA) using the Störmer-Verlet integrator defined as a composition method leads to the best accuracy. Although, relative to this method the VI-based generalized MCVA method offers computational savings when collisions are particularly sparse. Copyright © 2014 John Wiley & Sons, Ltd.

Received . . .

KEY WORDS: Störmer-Verlet, geometric integration, backwards error analysis, Hamiltonian systems, Lagrangian mechanics, impact dynamics, double pendulum

1. INTRODUCTION

Modeling and simulating mechanical systems subject to unilateral constraints is challenging due to the complex and nonsmooth nature of contact mechanics. Although at the microscale these systems' dynamics are dependent upon material deformation and elasticity, a common approach is to adopt a rigid body assumption for modeling and simulation [1, 2]. This assumption provides the benefit of a relatively low-dimensional description of system dynamics but at the cost of modeling errors created by disregarding the dynamics associated with elastic deformation. For engineering systems that exhibit minimal elastic deformation during operation, this tradeoff is highly favorable.

Working under the rigid body assumption there remains varied approaches to modeling nonsmooth systems. Barrier methods [3, 4] regularize contact impulses into smooth potential forces such that nonsmooth mechanics are approximated with smooth differential equations. Measure differential inclusions [5, 6, 7, 8] more accurately capture impulses by extending the classical theory for differential equations to admit set-valued forces. Alternatively, complementarity dynamical

*Correspondence to: Data Tactics Corp., 7901 Jones Branch Dr. #700, Arlington, VA, 22102 (dpekarek@data-tactics.com).

†This material is based upon work supported by the National Science Foundation under award CCF-0907869. Any opinions, findings, and conclusions or recommendations expressed in this material are those of the author(s) and do not necessarily reflect the views of the National Science Foundation.

systems [9, 10] capture impulses by pairing differential equations with complementarity conditions. Lastly there are variational models of contact, in which system dynamics may be captured as the solutions to variational inequalities [11, 12] or through stationarity principles [7, 13, 14]. As we are primarily concerned with the conservation properties associated with nonsmooth mechanics, variational models are a natural choice.

Regardless of modeling approach, it is typically intractable to identify analytical solutions to nonsmooth system dynamics and thus numerical simulation is required. Simulation methods for nonsmooth dynamics [15] are generally classified as either time-stepping schemes or event-driven schemes. Time-stepping schemes express discrete dynamics as a balance of discrete impulses (the integral of measure-valued quantities over time) and are capable of fixed advances in time regardless of changes in contact conditions. This is desirable in that time-stepping methods gracefully handle cases of dense accumulations of impact events. Schemes within this family [16, 17, 18, 19] may vary the quadrature used to compute impulses as well as the level (position or velocity) at which constraints are enforced. A comprehensive account of these variants is provided in [20]. Of particular note, relative to our work's focus on conservation laws and stabilization, is the symplectic time-stepping scheme provided in [21].

In contrast to time-stepping schemes, event-driven schemes [22, 23, 24] use adaptive time-stepping to identify precisely the time and configuration at which a change in contact occurs. This provides an opportunity for improved accuracy in resolving collisions, but makes these schemes only suitable for applications in which collisions a relatively sparse in time (a dense accumulation of impact events cannot be processed). We mention "an opportunity for improved accuracy" because it remains a problem that during event-driven simulations, maintaining conservation of energy through impacts is nontrivial. Figure 1, which depicts event-driven simulation results for a constrained double pendulum system undergoing perfectly elastic impacts, illustrates that even reasonable choices of a discrete time impact model–in this case the collision Verlet algorithm found in [22]–can introduce energy errors far greater than those associated with smooth dynamics simulations. Energy errors may enter during the process of identifying the collision time and configuration, or during the impulsive momentum update associated with impact. In either case, compounding these errors over multiple impacts effectively destabilizes a given simulation. Hence, within the context of event-driven simulations of systems with impacts sparse in time, we wish to address methods that counteract the above potential for destabilization.

In developing an event-driven scheme focused on energy stabilization and conservation laws, we build upon the prior work [14] that leverages variational nonsmooth mechanics and its extension to numerical methods through variational integrator (VI) theory [25, 26]. VIs [27, 28, 29] are generated through discrete variational principles rather than discretized equations of motion. The resulting integrators are considered attractive for their multiple structure preserving properties, including conservation of discrete momenta, a discrete symplectic form, and a modified Hamiltonian (MH) function. The last of these conservation laws is derived through a process known as backwards error analysis [30, 26], and is often cited as the reason for VIs' stable energy behavior when simulating smooth dynamics. As seen in the development of the event-driven modified collision Verlet algorithm (MCVA) [24], respecting MH conservation through discrete time impacts is the key to avoiding the aforementioned energy destabilization. However, the MCVA method is specific in its scope as it requires use of the Störmer-Verlet method and that the system of interest is conservative with a separable Hamiltonian.[†] In this work we produce a definition of the MH in terms of a general discrete Lagrangian, the central object in VI theory, that facilitates the creation of a general MH conservation based event-driven integrator for nonseparable, potentially nonconservative mechanical systems.

It is worth noting, while our expression of the MH in terms of the discrete Lagrangian is motivated by applications involving nonsmooth systems, in actuality it represents a more general contribution to structured integration theory. VIs can be considered a subset of the broader family of symplectic

[†]A separable Hamiltonian is one which can be expressed as $H(q,p) = T(p) + V(q)$. For such Hamiltonians, the vanishing of mixed partials, $\frac{\partial^2}{\partial p_i \partial q_j} H$, often simplifies integration methods.

DOI: 10.1002/nme

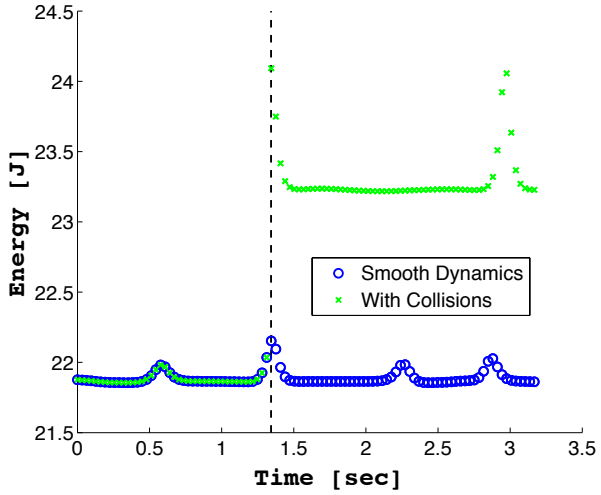

Figure 1. Energy behavior during event-driven simulations of a double pendulum system with and without collisions. When simulating smooth dynamics in the absence of impacts, energy is not exactly conserved but oscillates stably near its nominal value. During a simulation with impacts, resolution of a collision at $t = 1.34$ with the collision Verlet algorithm (see Subsection 4.1) causes a jump in energy of greater than 5%. Essentially, even a seemingly reasonable choice of discrete impact map can nullify the stable energy behavior associated with a given smooth integrator.

integration schemes. This family also contains as a subset discrete Hamiltonian integrators derived with mixed variable generating functions[‡,§]. Both integrator types, VIs and discrete Hamiltonian integrators, are supported by a rich discrete mechanics theory. Specifically, underpinning VIs is discrete Lagrangian mechanics characterized by a discretized Hamilton's principle [25, 26], and underpinning the discrete Hamiltonian integrators is discrete time Hamilton-Jacobi theory [26, 32]. Prior to this work, backwards error analysis for symplectic integrators has been conducted exclusively in the discrete Hamiltonian setting. Our expression of the MH in terms of the discrete Lagrangian for the first time links the tool of backwards error analysis and the discrete Lagrangian mechanics approach.

To be explicit, the contributions of this paper are as follows.

- Using backwards error analysis we establish a definition of the MH, the energetic quantity exactly preserved by a given integration method, for the VI family of methods.
- We explicitly define multiple versions of the Störmer-Verlet method, stemming from its interpretation as a VI or as a composition method, and their distinction when applied to nonseparable mechanical systems.
- We define an event-driven collision integration method, over the family of VIs, that conserves the MH to a user-specified order.
- We compare the aforementioned method to existing event-driven schemes in terms of discrete conservation laws, trajectory accuracy, computational effort, and admittance of nonconservative forcing.

In presenting these contributions, the structure of this paper is as follows. In Section 2 we introduce continuous-time representations of impact dynamics. In Section 3 we establish a backwards error analysis for VIs in terms of the discrete Lagrangian. In Section 4 we examine existing event-driven schemes for impact dynamics, namely the collision Verlet algorithm (CVA) [22], the variational

[‡]Generating functions offer a concise way to represent symplectic maps. That is, a given map is associated with a real function, which in turn generates the map through its partial derivatives. This process is discussed in Subsection 3.2. For further background, see [31].

[§]Actually, any symplectic scheme can be represented locally as either type, VI or discrete Hamiltonian integrator. However, the ease of representation may vary significantly, an issue which is revisited in Subsection 3.3.

DOI: 10.1002/nme

collision integrator (VCI) [14], and the MCVA [24]. We describe each algorithm's conservation properties and error order analyses, and generalize the MCVA to nonseparable systems and general choices of the discrete Lagrangian. In Section 5, we present simulation results comparing the various methods' computational performance in terms of conservation properties, trajectory errors as a function of initial condition and required computation time. Finally, our conclusions are given in Section 6 where we review our contributions in terms of generating new simulation methods, and provide a final comparison of existing simulation methods relative to the generalized MCVA.

2. IMPACT DYNAMICS

As a precursor to future sections regarding simulation methods, this section is concerned with continuous-time models of impact dynamics. With our focus on variational models [11, 12, 13, 14], dynamics are first derived in the Lagrangian setting by way of a nonsmooth Hamilton's variational principle. We assume system velocities and momenta are globally isomorphic, a property known as hyperregularity of the system Lagrangian. Under this assumption, the aforementioned variational impact dynamics have an equivalent description as a Hamiltonian system. Regardless of the choice of model, Lagrangian or Hamiltonian, these systems are symplectic and energy conserving. A precise description of these conservation laws in continuous time will aid us in evaluating simulation methods in discrete time.

2.1. Variational Lagrangian Impact Mechanics

Let us establish the following system model for the remainder of the paper. Consider a mechanical system with configuration space Q (assumed to be an n-dimensional smooth manifold with local coordinates q) and a Lagrangian $L : TQ \to \mathbb{R}$. This system is subject to a one-dimensional, holonomic, unilateral constraint defined by a smooth function $\phi : Q \to \mathbb{R}$ such that the feasible space of the system is $C = \{q \in Q \,|\, \phi(q) \geq 0\}$. We assume C is a submanifold with boundary in Q. Furthermore, we assume that 0 is a regular point of ϕ such that the boundary of C, $\partial C = \phi^{-1}(0)$, is a submanifold of codimension 1 in Q. Physically, ∂C is the set of contact configurations.

The variational approaches of [13, 14] demonstrate that system trajectories satisfy a space-time formulation of Hamilton's principle of least action. For a trajectory $q(t)$ that experiences a single impact at time t_i on the time interval $[0,T]$, this principle appears in its common form

$$\delta \int_0^T L(q(t),\dot{q}(t))\,dt = 0, \tag{1}$$

but in addition to the typical variations $\delta q(t)$ taken with respect to the trajectory, one takes variations δt_i with respect to the impact time[¶]. The resulting stationarity conditions associated with these variations require that for all $t \in [0,T]\backslash\{t_i\}$ the system evolves on C according to the standard Euler-Lagrange equations

$$\frac{d}{dt}\left(\frac{\partial L}{\partial \dot{q}}\right) - \frac{\partial L}{\partial q} = 0, \tag{2}$$

and at $t = t_i$ the system must satisfy the following impact conditions

$$\left[\frac{\partial L}{\partial \dot{q}}\right]_{t_i^-}^{t_i^+} = \lambda \nabla \phi(q_i), \tag{3}$$

$$E\Big|_{t_i^-}^{t_i^+} = 0, \tag{4}$$

[¶]The formulation in [14] opts to vary the parameterization of time as a whole, though away from the impact time t_i this only serves to generate redundant stationarity conditions.

DOI: 10.1002/nme

where $q_i = q(t_i^-) = q(t_i^+)$ is the system's configuration at impact and $E : TQ \to \mathbb{R}$ is the system's energy defined as

$$E(q,\dot{q}) = \dot{q}^T \frac{\partial L}{\partial \dot{q}} - L.$$

Essentially, the impact equations (3) and (4) indicate a conservation of momentum tangent[‖] to ∂C and a conservation of energy E across the impact.

2.2. Hamiltonian impact dynamics

In the discussions that follow it will often be helpful to reference a Hamiltonian formulation of impact dynamics. That is, we will occasionally discuss the prior subsection's impact mechanics with equivalent conditions in the Hamiltonian phase space T^*Q. To do this, let us assume here and henceforth that L is hyperregular [33, 25]. That is, the Legendre transform $\mathbb{F}L : TQ \to T^*Q$, defined in coordinates as

$$\mathbb{F}L : (q,\dot{q}) \mapsto (q,p) = \left(q, \frac{\partial L}{\partial \dot{q}}\right),$$

is a global isomorphism. In this case, our Lagrangian system can be extended to a Hamiltonian system on T^*Q with the Hamiltonian $H : T^*Q \to \mathbb{R}$ defined as

$$H = E \circ \mathbb{F}L^{-1}. \tag{5}$$

Using this H, we have Hamilton's equations

$$\dot{q} = \frac{\partial H}{\partial p}, \tag{6}$$

$$\dot{p} = -\frac{\partial H}{\partial q}, \tag{7}$$

which are equivalent to (2), and with appropriate substitutions the impact equations (3), (4) are stated equivalently as

$$p\big|_{t_i^-}^{t_i^+} = \lambda \nabla \phi(q_i), \tag{8}$$

$$H\big|_{t_i^-}^{t_i^+} = 0. \tag{9}$$

2.3. Conservation properties

The overall Lagrangian flow of the nonsmooth system is produced using the composition of two maps, the flow of the contact-free Euler-Lagrange equations and, in the presence of contact, the discrete impact equations. As each of these maps individually conserves E, the overall flow conserves E as well. Furthermore, it is shown in [14] that the overall nonsmooth flow exhibits conservation of an extended symplectic form $\Omega_L = -d\bar{\Theta}_L$, where

$$\bar{\Theta}_L = \frac{\partial L}{\partial \dot{q}} dq - E dt, \tag{10}$$

is a one form on $TQ \times \mathbb{R}$. When discussing integration algorithms in Section 4, we will analyze various methods' ability to provide exact or approximate discrete time versions of these conservation properties.

[‖] In fact, (3) can be expressed equivalently with a lower-dimensional projected momentum balance on $T^*\partial C$. We've written (3) on the overlying T^*C for ease of physical interpretation. The Lagrange multiplier term signifies an impulse delivered to the system.

DOI: 10.1002/nme

3. VARIATIONAL INTEGRATORS AND BACKWARDS ERROR ANALYSIS

Prior methods for simulating impacts, namely the CVA [22] and MCVA [24], rely exclusively on the Störmer-Verlet (SV) scheme [34] for integrating smooth dynamics away from impacts. It is well known that SV belongs to the family of VIs [26, 25]. In this section, we lay the foundation necessary for the simulation of impacts with any general VI method. Initially, we review multiple derivations of VIs, establishing a useful link between the discrete Lagrangian and an implicit mixed variable generating function definition of VIs. This leads to a central contribution of this paper, an expression for the modified Hamiltonian of a given VI directly in terms of its discrete Lagrangian.

3.1. Variational integrators generated with the discrete Lagrangian

VIs are generated with a discretization of Hamilton's principle (1). Central to the discretization, and the overall theory for VIs, is the introduction of a discrete Lagrangian, $L_d : Q \times Q \times \mathbb{R} \to \mathbb{R}$, which approximates the action on short time intervals using some user-prescribed quadrature. That is,

$$L_d(q_k, q_{k+1}, h) \approx \int_{kh}^{(k+1)h} L(q(t), \dot{q}(t))\, dt.$$

A summation of discrete Lagrangians provides a discrete version of Hamilton's principle,

$$\delta \sum_{k=0}^{N-1} L_d(q_k, q_{k+1}, h) = 0, \tag{11}$$

for all variations $\{\delta q_k\}_{k=0}^{N}$ with $\delta q_0 = \delta q_N = 0$. Stationarity in this discrete principle implies the discrete Euler-Lagrange equations

$$D_2 L_d(q_{k-1}, q_k, h) + D_1 L_d(q_k, q_{k+1}, h) = 0, \tag{12}$$

for all $k \in \{1, \ldots, N-1\}$, where the notation D_i indicates differentiation with respect to the i^{th} argument. For numerical integration purposes, we can view (12) as implicitly defining a discrete Lagrangian map $F_{L_d} : Q \times Q \to Q \times Q$ such that $F_{L_d}(q_{k-1}, q_k) = (q_k, q_{k+1})$.

VIs can also be viewed in the Hamiltonian setting. Following the definitions of [25], consider left and right discrete Legendre transforms $\mathbb{F}^+L_d, \mathbb{F}^-L_d : Q \times Q \times \mathbb{R} \to T^*Q$ defined in coordinates as

$$\mathbb{F}^+L_d : (q_0, q_1, h) \mapsto (q_1, p_1) = (q_1, D_2 L_d(q_0, q_1, h)), \tag{13}$$

$$\mathbb{F}^-L_d : (q_0, q_1, h) \mapsto (q_0, p_0) = (q_0, -D_1 L_d(q_0, q_1, h)). \tag{14}$$

Using these definitions, the discrete equations of motion (12) can be rewritten as a one-step method $\Phi_h : T^*Q \to T^*Q$. Specifically, using the definition

$$\Phi_h := \mathbb{F}^+L_d \circ \left(\mathbb{F}^-L_d\right)^{-1}, \tag{15}$$

we have $\Phi_h : (q_k, p_k) \mapsto (q_{k+1}, p_{k+1})$. Observe that, in notational agreement with [26], we have placed the argument h from $\mathbb{F}^{\pm}L_d$ as subscript on the mapping Φ. This does not exclude the possibility of varying the timestep, a practice that we will make use of in future sections, and that will be recorded with changes in this subscript.

It is also worth mentioning that under a discretized Lagrange-d'Alembert principle [25], VIs admit the structured inclusion of nonconservative external forces. Recall the statement of the continuous Lagrange-d'Alembert principle,

$$\delta \int_0^T L(q(t), \dot{q}(t))\, dt + \int_0^T f(t) \cdot \delta q(t)\, dt = 0,$$

where $f : \mathbb{R} \to T^*Q$ is some time-dependent generalized forcing. To discretize this principle, one must define left and right discrete forces, $f_k^-, f_k^+ \in T^*Q$ to provide an approximation of the virtual

DOI: 10.1002/nme

work. That is, using some specified quadrature f_k^- *and* f_k^+ must be defined to yield

$$f_k^- \cdot \delta q_k + f_k^+ \cdot \delta q_{k+1} \approx \int_{kh}^{(k+1)h} f(t) \cdot \delta q(t)\, dt.$$

With this definition, the discrete Lagrange-d'Alembert principle is stated,

$$\delta \sum_{k=0}^{N-1} L_d(q_k, q_{k+1}, h) + \sum_{k=0}^{N-1} f_k^- \cdot \delta q_k + f_k^+ \cdot \delta q_{k+1} = 0, \tag{16}$$

and produces as stationarity conditions the forced DEL equations,

$$D_2 L_d(q_{k-1}, q_k, h) + D_1 L_d(q_k, q_{k+1}, h) + f_{k-1}^+ + f_k^- = 0.$$

This structure indicates that VIs admit external forcing at the level of generating the integration scheme. For methods derived in the Hamiltonian setting [26], there is no parallel to 16. That is, there is no canonical method of incorporating external forces during generation of the integration scheme. Rather, for these methods forces must be inserted at the level of the discrete dynamics, through some modification of the one-step map Φ_h. Further, we mention that in the special case of VIs with explicit discrete Lagrangians, the statement of the discretized principle (16) above is explicit as well. This is a simplifying property that we will note in our coming discussion of integration methods.

3.2. Variational integrators derived with a mixed variable generating function

It is well known [26, 35, 32] that one can interpret the discrete Lagrangian L_d as a type one** generating function [31] for the map Φ_h. This provides as an immediate consequence that Φ_h is symplectic, since the general theory states that any sufficiently smooth and nondegenerate function $S : Q \times Q \to \mathbb{R}$ can be used to generate a symplectic map $(q_0, p_0) \mapsto (q_1, p_1)$ by using the relations

$$p_0 = -D_1 S(q_0, q_1), \tag{17}$$
$$p_1 = D_2 S(q_0, q_1). \tag{18}$$

This is not the only means by which to generate symplectic maps. In some cases it is advantageous to use so-called mixed variable generating functions, functions of type two or three (with respective arguments (q_0, p_1) or (q_1, p_0)). We will focus on the former. Given a sufficiently smooth type two function $\widehat{S}(q_0, p_1)$, the equations

$$p_0 = D_1 \widehat{S}(q_0, p_1), \tag{19}$$
$$q_1 = D_2 \widehat{S}(q_0, p_1). \tag{20}$$

define a symplectic map if $D_1 D_2 \widehat{S}$ is invertible. In [32], we see that with L_d and $\mathbb{F}^+ L_d$ we can implicitly construct the generating function $\widehat{S}$ that produces Φ_h. It is referred to as the right discrete Hamiltonian, $H_d^+ : T^*Q \times \mathbb{R} \to \mathbb{R}$, defined as

$$H_d^+(q_0, p_1, h) = p_1 \cdot q_1 - L_d(q_0, q_1, h), \tag{21}$$

in which q_1 appears as an implicit function of (q_0, p_1) through the relation

$$p_1 = D_2 L_d(q_0, q_1, h), \tag{22}$$

from $\mathbb{F}^+ L_d$. One can easily check that the mapping generated by substituting H_d^+ for $\widehat{S}$ in equations (19) and (20) is precisely the implicit Φ_h defined in (15).

**When generating a symplectic map, $\Phi : (q_0, p_0) \mapsto (q_1, p_1)$, a generating function is classified as type one if its arguments are (q_0, q_1).

DOI: 10.1002/nme

Structured integrators are typically generated as mappings near the identity, where $\widehat{S}$ takes the form

$$\widehat{S}(q_0, p_1) = p_1 \cdot q_0 + \bar{S}(q_0, p_1). \tag{23}$$

With some manipulation we see H_d^+ fits this form (i.e. $H_d^+ = \widehat{S}$) if one uses $\bar{S}(q_0, p_1) = h\eta(q_0, p_1)$, where

$$\eta(q_0, p_1) = p_1 \cdot \frac{q_1 - q_0}{h} - \frac{1}{h} L_d(q_0, q_1, h), \tag{24}$$

and once again q_1 is defined implicitly by equation (22). The form of η roughly appears as a discrete time calculation of the Hamiltonian using its definition in terms of the Lagrangian (5). This is not entirely surprising, as typically the $O(h)$ term for integration methods generated with a mixed variable generating function is $H(q_0, p_1)$, a property used to prove the following lemma.

Lemma 1
Given a hyperregular Lagrangian L and a discrete Lagrangian L_d that has order $s \geq 1$, the function $\eta : T^*Q \to \mathbb{R}$ in (24) and the Hamiltonian (5) corresponding to L satisfy

$$|\eta(q, p, h) - H(q, p)| = O(h),$$

for $(q, p) \in T^*Q$ and sufficiently small h. That is, η and H are accurate to first order.

Proof
This follows from two existing results. First, in Theorem 2.3.1 of [25], we have that L_d is order $s \geq 1$ implies that the associated one-step map Φ_h is of order $s \geq 1$ as well. Second, in Section VI.5.4 of [26] we see that an $O(h^s)$ perturbation in given method's generating function $\widehat{S}$ leads to an $O(h^{s+1})$ perturbation in the method's solution of the Hamilton-Jacobi partial differential equation. As $tH(q, p)$ is the leading term in the exact solution of this PDE we have that for any first order method Φ_h (i.e. with $s \geq 1$) generated with some $\widehat{S}$, the quantity $\frac{1}{h}\widehat{S}$ agrees with H to first order. Hence, $|\eta(q, p, h) - H(q, p)| = O(h)$. □

The purpose of this lemma is twofold. First, it establishes some intuition regarding the accuracy of η as an approximation to H. Second, it provides that first order accuracy, as a property associated with generating functions, is preserved when moving between the discrete Lagrangian and discrete Hamiltonian settings. An extension of this relationship to higher orders is anticipated, but not undertaken in this work.

3.3. Störmer-Verlet as a variational integrator

The SV method [34] serves as an attractive option for separable systems, as it provides a second order accurate, explicit integrator in that setting. In the aforementioned work, several interpretations of the method are given, including its structure as a composition method and as a variational integrator. When applied to nonseparable systems, these interpretations of SV are no longer coincident, and thus we make the following comments about the generally different versions of the method.

While the structure of the SV method can be interpreted in several ways, we begin with its definition as a composition method. To do so we must first define the pair of symplectic Euler methods, denoted SE1 and SE2, that are VIs in their own right and generated respectively with the type one equations (17), (18) applied to the discrete Lagrangians

$$L_d^{\mathrm{SE1}}(q_k, q_{k+1}, h) = hL\left(q_k, \frac{q_{k+1} - q_k}{h}\right),$$
$$L_d^{\mathrm{SE2}}(q_k, q_{k+1}, h) = hL\left(q_{k+1}, \frac{q_{k+1} - q_k}{h}\right).$$

DOI: 10.1002/nme

The one-s tep maps, Φ_h^{SE1} and Φ_h^{SE2}, produced by the above discrete Lagrangians through (15) have the relation

$$\Phi_h^{\mathrm{SE1}} \circ \Phi_{-h}^{\mathrm{SE2}} = \mathbb{I},$$

where $\mathbb{I}$ symbolizes the identity mapping. Being so, these methods are referred to as adjoint. Using these definitions, the pair of SV methods, denoted SVA and SVB, can be defined as

$$\Phi_h^{\mathrm{SVA}} = \Phi_{h/2}^{\mathrm{SE2}} \circ \Phi_{h/2}^{\mathrm{SE1}},$$
$$\Phi_h^{\mathrm{SVB}} = \Phi_{h/2}^{\mathrm{SE1}} \circ \Phi_{h/2}^{\mathrm{SE2}}.$$

Note that if the methods are appropriately initialized a half timestep apart, SVA and SVB can be said to produce equivalent results. That is, we have the identity

$$\Phi_{Nh}^{\mathrm{SVA}} = \Phi_{h/2}^{\mathrm{SE2}} \circ \Phi_{(N-1)h}^{\mathrm{SVB}} \circ \Phi_{h/2}^{\mathrm{SE1}},$$

for any positive integer N. One can also derive SV from a mixed variable generating function. In [34], it is mentioned that (23) produces SVA through the use of

$$\begin{aligned}\bar{S}^{\mathrm{SVA}}(q_0, p_1) = &\frac{h}{2}\left(H(q_0, p_{1/2}) + H(q_1, p_{1/2})\right) \\ &- \frac{h^2}{4} D_1 H(q_1, p_{1/2}) \cdot \left(D_2 H(q_0, p_{1/2}) + D_2 H(q_1, p_{1/2})\right),\end{aligned} \tag{25}$$

where $p_{1/2}$ and q_1 above are viewed as implicit functions of q_0 and p_1 by the SVA equations. Lastly, though it's not particularly compact, SVA and SVB can also be defined as resulting from the respective discrete Lagrangians

$$L_d^{\mathrm{SVA}}(q_k, q_{k+1}, h) = \min_{q_{k+1/2}} \left[\frac{h}{2} L\left(q_k, \frac{q_{k+1/2} - q_k}{h}\right) + \frac{h}{2} L\left(q_{k+1}, \frac{q_{k+1} - q_{k+1/2}}{h}\right)\right],$$
$$L_d^{\mathrm{SVB}}(q_k, q_{k+1}, h) = \min_{q_{k+1/2}} \left[\frac{h}{2} L\left(q_{k+1/2}, \frac{q_{k+1/2} - q_k}{h}\right) + \frac{h}{2} L\left(q_{k+1/2}, \frac{q_{k+1} - q_{k+1/2}}{h}\right)\right].$$

The discrete Lagrangians above come in contrast to several existing sources [36, 34, 25, 26] characterizing SV as a VI. In these works, which only discuss the method when applied to separable systems, the discrete Lagrangian for SV is given as

$$L_d^{\mathrm{SVC}}(q_k, q_{k+1}, h) = \frac{h}{2}\left[L\left(q_k, \frac{q_{k+1} - q_k}{h}\right) + L\left(q_{k+1}, \frac{q_{k+1} - q_k}{h}\right)\right]. \tag{26}$$

The corresponding integrator, in the separable case, is equivalent to SVA. That is, the commutative relation shown in figure 2 holds. For general, nonseparable systems such a diagram still exists, but the mixed variable generating function $\widehat{S}$ and one-step method Φ_h on the right hand side are distinct from the SVA method. Thus, in this in this work we denote the VI produced by (26) as SVC.

The SVC integrator serves as a motivating example for our focus on conducting backwards error analysis in terms of the discrete Lagrangian. Many VIs[††] are represented with comparable ease in the Hamiltonian setting. That is, they admit some mixed variable generating function[‡‡] representation of the same complexity (i.e. explicit, implicit) as the discrete Lagrangian. SVC has an explicit discrete Lagrangian, which we've mentioned yields an explicit statement of the discrete Lagrange principle in applications with external forcing. However, the method does not have a corresponding simple generating function, seeming to indicate SVC is best suited for representation as a VI. Certainly we cannot claim that all symplectic methods are best represented as VIs, but SVC serves as an indication that some methods are. In turn, the following development of a backwards error analysis for VIs in terms of the discrete Lagrangian is particularly useful for such methods.

[††] For instance, the symplectic Euler pair, SVA, SVB, the implicit midpoint rule, and the general family of symplectic partitioned Runge-Kutta methods.

[‡‡] This function may not necessarily be type two.

DOI: 10.1002/nme

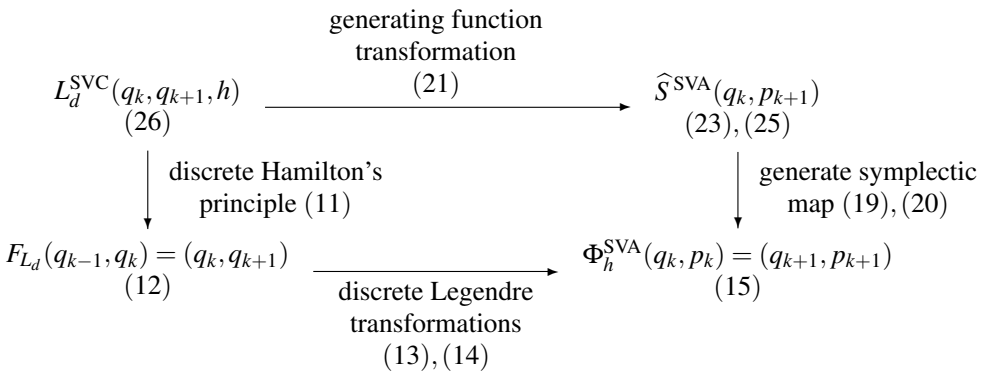

Figure 2. When integrating separable mechanical systems the following commutativity diagram connects the discrete Lagrangian for SVC, L_d^{SVC}, and the one-step method associated with SVA, Φ_h^{SVA}. One can arrive at the one-step method by converting L_d^{SVC} into a mixed variable generating function (top right) or by performing a discrete Legendre transformation on the DEL equations associated with L_d^{SVC} (lower left).

3.4. Backwards error analysis

VIs do not exactly conserve energy but do, as stated prior, exhibit stable energy behavior. The guarantee of this stability can be demonstrated via backwards error analysis, which shows that the discrete flow Φ_h for any symplectic one-step method provides the exact solution to a modified differential equation which is also Hamiltonian [30, 26]. This implies that every VI has associated with it a modified Hamiltonian (MH) as a conserved quantity. Furthermore, it is true in general that the MH differs from that of the system being simulated by $\mathrm{O}(h^r)$ where r is the order of the VI in use [34]. We provide the following result relating the MH for a given VI to its discrete Lagrangian L_d.

Theorem 2
Assume we are given a consistent discrete Lagrangian L_d with the corresponding one-step map Φ_h and right discrete Hamiltonian H_d^+. The application of Φ_h to a hyperregular Lagrangian system L provides the exact solution to a modified equation that is a Hamiltonian system with

$$\widetilde{H}(q,p) = \eta(q,p) + hH_2(q,p) + h^2H_3(q,p) + \ldots, \tag{27}$$

where $\eta(q,p)$ is as defined in (24) and the terms H_i are composed using higher derivatives of η. The H_i are smooth on any open set $B \subset T^*Q$ in which H_d^+ is smooth and generates Φ_h.

Proof
We practice the same proof by construction as given in [26] (Thm IX.3.2). That is, the terms H_i are defined by equating the VI's generating function $\bar{S}(q,p) = h\eta(q,p)$ with a continuous-time solution $\widetilde{S}(q,p,t)$ of the Hamilton-Jacobi PDE

$$\frac{\partial \widetilde{S}}{\partial t}(q,p,t) = \widetilde{H}\left(q + \frac{\partial \widetilde{S}}{\partial p}(q,p,t), p\right), \tag{28}$$

$$\widetilde{S}(q,p,0) = 0. \tag{29}$$

Though it is not shown explicitly in the following derivation, it is important to remember η is a function of L_d and as such $\widetilde{S}$ and $\widetilde{H}$ will be as well.

We specifically seek a continuous-time solution $\widetilde{S}(q,p,t)$ with the property $\widetilde{S}(q,p,h) = h\eta(q,p)$. Prior to enforcing this property we will doubly expand $\widetilde{S}$, first in powers of t and then in powers of

DOI: 10.1002/nme

h. The first expansion appears as

$$\widetilde{S}(q,p,t) = t\widetilde{S}_1(q,p,h) + t^2\widetilde{S}_2(q,p,h) + t^3\widetilde{S}_3(q,p,h) + \ldots,$$

and each $\widetilde{S}_j(q,p,h)$ can be defined by comparing like powers of h when $t = h$ in (28). The first few terms are

$$\begin{aligned}
\widetilde{S}_1(q,p,h) &= \widetilde{H}(q,p), \\
2\widetilde{S}_2(q,p,h) &= \left(\frac{\partial \widetilde{H}}{\partial q}\cdot\frac{\partial \widetilde{S}_1}{\partial p}\right)(q,p,h), \\
3\widetilde{S}_3(q,p,h) &= \left(\frac{\partial \widetilde{H}}{\partial q}\cdot\frac{\partial \widetilde{S}_2}{\partial p}\right)(q,p,h) + \frac{1}{2}\left(\frac{\partial^2 \widetilde{H}}{\partial q^2}\cdot\left(\frac{\partial \widetilde{S}_1}{\partial p},\frac{\partial \widetilde{S}_1}{\partial p}\right)\right)(q,p,h).
\end{aligned} \tag{30}$$

Now for the second expansion, each $\widetilde{S}_j(q,p,h)$ is expanded as

$$\widetilde{S}_j(q,p,t) = \widetilde{S}_{j1}(q,p) + h\widetilde{S}_{j2}(q,p) + h^2\widetilde{S}_{j3}(q,p) + \ldots,$$

such that in total we have

$$\widetilde{S}(q,p,h) = \sum_{j,k} h^j h^{k-1}\widetilde{S}_{jk}(q,p).$$

Returning to the desired equivalence $\widetilde{S}(q,p,h) = h\eta(q,p)$, we now have $\widetilde{S}_{11}(q,p) = \eta(q,p)$ (indicating η is the $O(1)$ term in $\widetilde{H}$, as shown in the statement of the theorem) and

$$\sum_{k=1}^{i} \widetilde{S}_{k,i+1-k}(q,p) = 0,$$

for $i > 1$. The current set of equations is underdetermined, but can be completed with relations provided by inserting the individual $\widetilde{S}_j$ expansions and equation (27) for $\widetilde{H}$ into (30). Comparing like powers of h in this case, reveals $\widetilde{S}_{1i} = H_i$ for $i > 2$ and the general $\widetilde{S}_{jk}$ exist as functions of derivatives of H_ℓ with $\ell < k$. To isolate the desired $\widetilde{S}_{1i} = H_i$, one must employ recursive calculations of first a term H_i from η and its derivatives, followed by quantities $\widetilde{S}_{jk}$ ($j \neq 1$) as a function of terms H_ℓ ($\ell < k$) and their derivatives. □

As we stressed when beginning the proof of Theorem 2, the quality that differentiates it from the results in [26] is that all of the significant quantities η, $\widetilde{S}_{jk}$, and H_i are computable with the discrete Lagrangian L_d. We expand upon this computational accessibility in Appendix A by providing explicit expressions for the terms H_2, H_3, and H_4 necessary for a third order truncation of the MH.

3.5. Multiple interpretations of symplecticity

We have already made mention of the symplecticity of VIs as a result of their construction using generating functions. This establishes that the one-step map Φ_h associated with any VI conserves a canonical Hamiltonian symplectic form [33]. Using the backwards error analysis we have established, the symplectic form conserved must precisely be the continuous-time form associated with a given method's Hamiltonian modified equations. We have yet to mention an alternative view [25] that the symplecticity of VI methods may be viewed as the conservation of the discrete symplectic form $\Omega_{L_d} = d\Theta^+_{L_d} = d\Theta^-_{L_d}$, where

$$\begin{aligned}
\Theta^+_{L_d}(q_k,q_{k+1}) &= D_2L_d(q_k,q_{k+1})dq_{k+1}, \\
\Theta^-_{L_d}(q_k,q_{k+1}) &= -D_1L_d(q_k,q_{k+1})dq_k,
\end{aligned}$$

are one-forms on $Q \times Q$. Both of these notions of symplecticity, continuous and discrete, will arise in our analysis of impact integration methods.

DOI: 10.1002/nme

4. STRUCTURED INTEGRATION METHODS FOR IMPACTS

We now consider the task of numerically integrating the nonsmooth mechanics presented in Section 2. We will review three of the simulation methods discussed in [24]: CVA, VCI, and MCVA. Each of these methods falls into the class of event-driven collision integrators, which use adaptive timestepping to resolve impact dynamics at configurations on the contact set ∂C. Beyond the review of existing collision integrators, we will utilize our development of backwards error analysis for VIs to generalize the MCVA to nonseparable systems and any choice of discrete Lagrangian. For each integration method, we discuss the existence or lack of discrete time symplecticity and energy conservation.

4.1. Collision Verlet algorithm

As defined in [22], the collision Verlet algorithm (CVA) uses fixed timestep SV[§§] for smooth integration between collisions and a combination of partial timestepping and impulsive momentum updates to resolve collisions. To determine if a given time step contains one or more collisions, one must compute the partial timestep to encounter the next collision defined as

$$\text{CollisionTime}\,[\Phi, q, p] := \Big\{ \tau > 0 \mid (\tilde{q}, \tilde{p}) = \Phi_\tau(q,p),\ \phi(\tilde{q}) = 0 \Big\}.$$

For the systems of interest in [22], collision times could be computed as the solution to a quartic equation. Thus, in the original CVA a check for a collision time $\tau < h$ was performed in every timestep. As we consider nonseparable mechanical systems, for which searching for collision times is often more costly, our implementation of CVA makes use of an additional precondition[¶¶] that must be satisfied before instantiating a root-finding search for a collision. The precondition is simply

$$\phi(\tilde{q}) < 0, \tag{31}$$

where $(\tilde{q}, \tilde{p}) = \Phi_h^{\text{SVC}}(q,p)$, and qualitatively this is the requirement that fixed timestepping must yield an inadmissible configuration to signify that a collision has occurred.

As a quick aside, let us briefly comment on the affects of the aforementioned partial timestepping and root finding on the accuracy of event-driven simulations. In [23] it is proven, for the specific case of an oscillator subject to a linear unilateral constraint, that the root finding to determine a collision time τ must be at least $O(h^4)$ to preserve the fourth order accuracy of a given discrete flow map when handling the nonsmooth case. Analysis of our more general nonsmooth systems, in which the unilateral constraint is a nonlinear function $\phi(q)$, is significantly more complex. Though we do not pursue an explicit analysis here, we are inclined to mention that it is our practice and recommendation to enforce that partial timestep computations are several orders more accurate than the order of the integrator in use. This is not unlike the practices recommended for the structured integration of smooth mechanical systems [26], in which implicit flow maps and root finding are also commonly at play.

Now, if the precondition (31) identifies a timestep in which a collision occurs, one must compute the time to collision $\tau \leq h$ and evolve the system to the impact configuration using Φ_τ^{SVC}. At this stage, CVA specifies that one computes the post impact phase by solving the continuous-time impact equations (8), (9). We denote the solution of these equations as a reset map $R^{\text{CVA}} : T^*Q \to T^*Q$, where the mapping

$$(q(t_i^+), p(t_i^+)) = R^{\text{CVA}}(q(t_i^-), p(t^-)), \tag{32}$$

[§§] As [22] deals with separable systems, the original implementation of CVA is ambiguous in distinguishing between the use of SVA and SVC. In the remainder of this work we adopt SVC when applying CVA to non separable systems.

[¶¶] This precondition is borrowed from the Variational Collision Integrator covered in Subsection 4.2.

DOI: 10.1002/nme

provides

$$\begin{aligned} q(t_i^+) &= q(t_i^-), \\ p(t_i^+) &= p(t_i^-) + \lambda \nabla \phi(q(t_i^-)), \\ H(q(t_i^+), p(t_i^+)) &= H(q(t_i^-), p(t_i^-)), \\ p(t_i^+) &\neq p(t_i^-). \end{aligned}$$

With the above definitions, our implementation of CVA fits the general form*** of the Event-driven Collision Integration provided in Algorithm 1. Specifically, CVA is obtained by substituting $\Phi^{\text{full}} = \Phi^{\text{partial}} = \Phi^{\text{SVC}}$ and $R^{\text{reset}} = R^{\text{CVA}}$ into the algorithm.

Algorithm 1 Event-driven Collision Integration (given maps Φ^{full}, Φ^{partial}, and R^{reset})

$(\tilde{q}_{i+1}, \tilde{p}_{i+1}) = \Phi_h^{\text{full}}(q_i, p_i)$
if $\phi(\tilde{q}_{i+1}) > 0$ **then**
  $(q_{i+1}, p_{i+1}) = (\tilde{q}_{i+1}, \tilde{p}_{i+1})$
else
  $(\hat{q}_0, \hat{p}_0) = (q_i, p_i)$
  $\tau_{\max} = h$ and $k = 0$
  while $\tau_{\max} > 0$ **do**
    $\Delta\tau_k = \text{CollisionTime}\left[\Phi^{\text{partial}}, \hat{q}_k, \hat{p}_k\right]$
    $\left(\tilde{\tilde{q}}_{k+1}, \tilde{\tilde{p}}_{k+1}\right) = \Phi_{\Delta\tau_k}^{\text{partial}}(\hat{q}_k, \hat{p}_k)$
    if "Collision" **then**
      $(\hat{q}_{k+1}, \hat{p}_{k+1}) = R^{\text{reset}}\left(\tilde{\tilde{q}}_{k+1}, \tilde{\tilde{p}}_{k+1}\right)$
    else
      $(\hat{q}_{k+1}, \hat{p}_{k+1}) = \left(\tilde{\tilde{q}}_{k+1}, \tilde{\tilde{p}}_{k+1}\right)$
    end if
    $\tau_{\max} = \tau_{\max} - \Delta\tau_k$ and $k = k+1$
  end while
  $(q_{i+1}, p_{i+1}) = (\hat{q}_k, \hat{p}_k)$
end if

It may seem that a reset map derived from the continuous-time impact equations (8), (9) seems reasonable, but from a conserved quantities viewpoint this choice breaks the structure of the impact-free integration. The Hamiltonian, H, is not conserved exactly by the map Φ_h^{SVC}, and thus its conservation at a point in time with (9) yields no overlying discrete time energy conservation law. Furthermore, the extended symplectic form Ω_L that is conserved by the continuous-time impact map is not conserved exactly by Φ_h^{SVC}, so CVA provides no overall notion of symplecticity either. Of the integration methods we will discuss, CVA is the only one involving explicit impact equations†††, but at the apparent cost of ignoring SV's discrete time conservation laws.

4.2. Variational collision integrator

Rather than simply inserting impact equations into the integration process, the variational collision integrator (VCI) of [14] is developed through a discretization of the nonsmooth Hamilton's principle (1). As it happens, when using the discrete Lagrangian associated with SVC the stationarity conditions derived for the VCI integrator largely overlap with conditions imposed by CVA. The two schemes are in agreement in all aspects except the definition of the reset map R^{reset}. Rather than

***Given a large overlap in structure the numerical schemes we will discuss, one general algorithm is presented that permits variations by changes in the choice of three maps Φ^{full}, Φ^{partial}, and R^{reset}.

†††In our coming example, the Lagrangian is quadratic in $\dot{q}$. As such, it admits an explicit definition of the mapping (32).

Prepared using nmeauth.cls
DOI: 10.1002/nme

the map (32), VCI applies its own reset map $R^{\text{VCI}} : T^*Q \to T^*Q$ with

$$(q(t_i^+), p(t_i^+)) = R^{\text{VCI}}(q(t_i^-), p(t_i^-)), \tag{33}$$

providing the following

$$\begin{aligned}
q(t_i^+) &= q(t_i^-),\\
p(t_i^+) &= p(t_i^-) + \lambda \nabla \phi(q(t_i^-)),\\
-D_3 L_d^{\text{SVC}}\left(q(t_{i-1}), q(t_i^-), \Delta\tau_k\right) &= -D_3 L_d^{\text{SVC}}\left(q(t_i^+), q(t_{i+1}), \tau_{\max}\right),\\
(q(t_i^+), p(t_i^+)) &= \mathbb{F}^- L_d^{\text{SVC}}\left(q(t_i^+), q(t_{i+1}), \tau_{\max}\right),\\
(q(t_i^-), p(t_i^-)) &= \mathbb{F}^+ L_d^{\text{SVC}}\left(q(t_{i-1}), q(t_i^-), \Delta\tau_k\right),\\
p(t_i^+) &\neq p(t_i^-).
\end{aligned}$$

That is, the reset map for VCI replaces the use of the continuous-time Hamiltonian, H, with the discrete energy function, $-D_3 L_d : Q \times Q \times \mathbb{R}$. The use of this function as a discretization of E has been established prior in works concerned with space-time discrete Lagrangian structures [37, 25].

In the context of the general scheme of Algorithm 1, VCI is obtained by substituting $\Phi^{\text{full}} = \Phi^{\text{partial}} = \Phi^{\text{SVC}}$ and $R^{\text{reset}} = R^{\text{VCI}}$. VCI shares with CVA the property that the energetic quantity conserved through collisions does not match a conserved quantity of Φ_h^{SVC}, and thus no overall discrete time energy conservation law persists. However, it is shown in [14] that the impact equations for VCI do conserve Ω_{L_d} and thus VCI is an exact symplectic method.

4.3. Modified collision Verlet algorithm

Based on the discrete time preservation of truncated MHs as a higher order invariant, the modified collision Verlet algorithm (MCVA) was developed in [24]. It is noted there, the CVA and VCI algorithms conflict with the existing backwards error analysis for SV both in terms of their partial timestepping to and from impact and in terms of their respective impact equations. Ideally, a method would exist to perform these steps while exactly solving the modified equations and exactly conserving the MH. To date no such method exists, due to the infinite dimensional nature of the series expansion of the MH, and thus MCVA focuses on preserving the MH to a specified order.

In the task of partial timestepping to and from impact configurations, MCVA specifies the use of a higher order integrator applied to the Hamiltonian dynamics associated with a truncated MH. In the specific examples of [24], a fourth-order Gauss integration scheme is used to solve the Hamilton's equations associated with a fourth-order truncation of $\widetilde{H}$. We will denote this MH truncation as

$$\widetilde{H}^{O(h^4)}(q,p) = \eta(q,p) + hH_2(q,p) + h^2 H_3(q,p) + h^3 H_4(q,p).$$

Additionally, we will denote higher order flow maps by their order of accuracy and apply a tilde to indicate the map is integrating the dynamics of a truncated MH. So fourth-order Gauss integration of the dynamics associated with $\widetilde{H}^{O(h^4)}$ is denoted $\widetilde{\Phi}^{O(h^4)}$. If it's not apparent, the application of a fourth order method in this manner conserves both $\widetilde{H}^{O(h^4)}$ and $\widetilde{H}$ to fourth order.

MCVA also makes use of the truncation $\widetilde{H}^{O(h^4)}$ to define its reset map. To be explicit, $R^{\text{MCVA}} : T^*Q \to T^*Q$ is the mapping

$$(q(t_i^+), p(t_i^+)) = R^{\text{MCVA}}(q(t_i^-), p(t^-)), \tag{34}$$

that provides

$$\begin{aligned}
q(t_i^+) &= q(t_i^-),\\
p(t_i^+) &= p(t_i^-) + \lambda \nabla \phi(q(t_i^-)),\\
\widetilde{H}^{O(h^4)}(q(t_i^+), p(t_i^+), h) &= \widetilde{H}^{O(h^4)}(q(t_i^-), p(t_i^-), h),\\
p(t_i^+) &\neq p(t_i^-).
\end{aligned}$$

Prepared using nmeauth.cls
DOI: 10.1002/nme

With all of the definitions above, we have that MCVA is equivalent to Algorithm 1 under the substitutions $\Phi^{\text{full}} = \Phi^{\text{SVA}}$, $\Phi^{\text{partial}} = \widetilde{\Phi}^{O(h^4)}$, and $R^{\text{reset}} = R^{\text{MCVA}}$. MCVA does not provide any exact discrete energy conservation or discrete time symplecticity. However, the above application of MCVA does solve the modified equations to fourth order, and thus can be said to preserve the associated MH and associated extended symplectic form Ω_L to fourth order.

4.4. Generalized MCVA

Using the developments in the prior Section 3, when given a discrete Lagrangian, L_d, one can calculate any truncation of the associated MH and its Hamilton's equations in terms of L_d. As a direct result, we have generalized the MCVA integration scheme to any VI, any order of MH truncation, and any choice of higher order integrator. Further, this generalization can solve the modified equations, conserve the MH, and conserve an extended symplectic form Ω_L to a user specified order of accuracy. Specifically, to attain solutions of order s to the modified equations associated with a VI with discrete Lagrangian L_d, one simply needs to derive the Hamilton's equations associated with a MH truncation $\widetilde{H}^{O(h^s)}$ (equations that will be defined in terms of L_d) and perform partial timestepping using an s-order integrator $\widetilde{\Phi}^{O(h^s)}$. In the context of Algorithm 1, a general MCVA scheme for a given L_d and order s is produced with $\Phi^{\text{full}} = \Phi$ (the one-step map associated with a chosen L_d), $\Phi^{\text{partial}} = \widetilde{\Phi}^{O(h^s)}$ (defined with the user's choice of s-order integrator), and R^{reset} taking the same structure as R^{MCVA} but now requiring conservation of $\widetilde{H}^{O(h^s)}$.

5. SIMULATION RESULTS AND COMPARISONS

In the following we compare the methods of Section 4 during simulation of a vertical cart-pendulum with impacts. We model the nonsmooth mechanics of this system according to the elastic impact theory of Section 2. Simulation results are presented for each of the methods in Section 3, including the generalized MCVA as defined with the SVC variational integrator. Simulations are evaluated in terms of their respective error in resulting trajectories and, in the case of the MH-based methods, their average computation time. Further, we discuss an important distinction between the MCVA and generalized MCVA in terms of the order of accuracy attainable with a fixed number of derivatives of the generating function $\bar{S}$ (or equivalently η).

5.1. The vertical cart-pendulum with impacts

Consider a cart of mass m_1 affixed to a vertical track. Attached to the center of the cart with an inertialess rod of length L is a pendular point mass m_2. The configuration space for this cart-pendulum is $Q = \mathbb{R} \times S^1$ with coordinates $q = (y, \theta)$, where y is the height of the cart and θ is the angle of the pendulum with respect to vertical. Under the influence of gravity, g, the cart-pendulum's Lagrangian is

$$L(q, \dot{q}) = \frac{1}{2} \dot{q}^T M(q) \dot{q} - V(q), \tag{35}$$

where

$$M(q) = \begin{bmatrix} m_1 + m_2 & m_2 L \sin\theta \\ m_2 L \sin\theta & m_2 L^2 \end{bmatrix},$$
$$V(q) = (m_1 + m_2) g y - m_2 g L \cos\theta.$$

We note that

$$\det(M(q)) = m_2 L^2 (m_1 + m_2 \cos^2\theta)),$$

which never vanishes on Q for positive m_1 and m_2. Thus the cart-pendulum's Lagrangian is hyperregular. We will subject the system to the unilateral constraint

$$\phi(q) = y,$$

DOI: 10.1002/nme

Table I. Summary of properties of impact integration methods. MCVAC is the only method under consideration with all of the listed features.

Method	Conserves Associated MH	Symplectic (to specified accuracy)	Explicit Discrete Lagrangian (simplifying disc. Lagrange-d'Alembert princ.)
CVA			✓
VCI		✓ (exact)	✓
MCVAA	✓	✓	
MCVAC	✓	✓	✓

requiring that the vertical position of the cart remains positive. It is assumed that the pendulum does not physically interact with the presence of the constraint surface.

5.2. Cart-pendulum nonsmooth simulation results

With regards to the unilaterally constrained vertical cart-pendulum system, we provide simulation results for the following methods:

1. CVA (of Subsection 4.1),
2. VCI (of Subsection 4.2),
3. MCVAA, which we use to denote MCVA (of Subsection 4.3) with SVA for its smooth integration and impact equations defined with a fourth order MH trunction, $\widetilde{H}^{O(h^4)}$, and fourth order Gaussian quadrature for $\widetilde{\Phi}^{O(h^4)}$,
4. MCVAC, which we use to denote the generalized MCVA (of Subsection 4.4) with SVC for its smooth integration and impact equations defined with a third order MH trunction, $\widetilde{H}^{O(h^3)}$, and fourth order Gaussian quadrature for $\widetilde{\Phi}^{O(h^4)}$.

For a summary of the different properties of these methods, as described in the previous Section 4, refer to Table I. The choice to specify the MCVAC simulations with third-order modified Hamiltonian conservation, rather than fourth order conservation as in the MCVAA simulations, was not arbitrary. Rather, the methods were specified such that they require an equivalent number of derivatives of the generating function $\bar{S}$. For MCVAC, to calculate $\widetilde{H}^{O(h^3)}$ required all first and second derivatives of $\eta = \frac{1}{h}\bar{S}^{\mathrm{SVC}}$. In the case of MCVAA, we also used only first and second derivatives of $\bar{S}^{\mathrm{SVA}}$. However, MCVAA benefits from a well-known theorem [26] which provides that for symmetric Φ_h the terms in the MH associated with odd powers of h must vanish. This means that for SVA, on which MCVAA is based, we have $H_4 = 0$ and $\widetilde{H}^{O(h^3)} = \widetilde{H}^{O(h^4)}$. It happens that SVC, on which our version of MCVAC is based, also has a symmetric one-step map, Φ_h^{SVC}. However, the aforementioned theorem cannot apply because the leading term in our MH expansion for SVC is η and not H. That methods derived in the Hamiltonian setting achieve 'bonus' orders of MH accuracy indicates one drawback to the VI-centered approach to impact integration.

In all simulations, system parameters were fixed as $m_1 = 1$, $m_2 = 0.2$, $L = 2$, and $g = 10$. For each of the four methods, the "full" timestep h was varied between $3.2\mathrm{E}-2$ and $1\mathrm{E}-2$[‡‡‡] With the above parameters, we explored a one-parameter family of initial conditions. Specifically, using linear samples of a parameter $\beta \in [3.2, 5.2]$, we derived associated initial conditions with a mapping $\Xi : \mathbb{R} \to T^*Q$ defined as

$$\Xi(\beta) = \mathbb{F}L([\beta, 0], [0, 3.5 - 0.18\beta]).$$

[‡‡‡]A timestep of $3.2\mathrm{E}-2$ might seem arbitrary, but was actually specifically chosen for its relative closeness to $\sqrt{10}\mathrm{E}-2$. This choice displays the second-order accuracy of the SV method very clearly in our given figures. That is, when comparing simulations using timesteps $h = 3.2\mathrm{E}-2$ and $h = 1\mathrm{E}-2$ a second-order method provides trajectories that differ in accuracy by one order of magnitude. This difference of a single power of ten is easily identifiable with the logarithmic scale we use.

Prepared using nmeauth.cls
DOI: 10.1002/nme

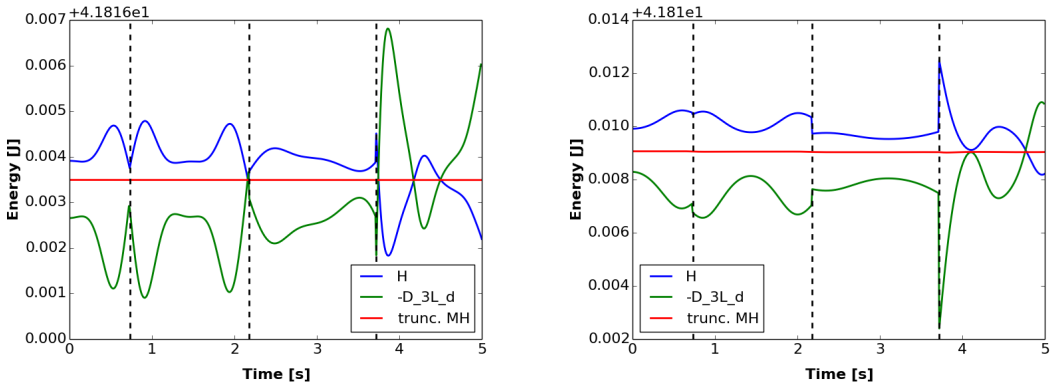

Figure 3. For sample MCVAA (left) and MCVAC (right) cart-pendulum simulations, the resulting time evolution of three different representations of system energy: the Hamiltonian H, the discrete energy $-D_3L_d$, and the truncated modified Hamiltonian. Impact times are denoted with the vertical dashed lines. Though the system's continuous-time dynamics are derived from H, both simulations best conserve the truncated MH.

This targeted sampling of initial conditions covers a spectrum of total system energies between 41 and 65 J, and was chosen specifically to offer that results have a smooth dependence on initial conditions. In general simulations of the cart-pendulum, impact events sometimes act as saddle points that greatly amplify small differences between trajectories. This sensitivity to local errors is natural for nonsmooth systems, but is a corrupting force when attempting to compare simulation methods. By focusing on trajectories associated with initial conditions $(q_0, p_0) = \Xi(\beta)$, we have avoided saddle points and offer a fair comparison of methods.

As a precursor to our comparisons of model accuracy, let us first examine Figure 3 which shows the time evolution of energy functions for each an MCVAA simulation and an MCVAC simulation. Specifically, the depicted results are from simulations using the initial conditions $(q_0, p_0) = \Xi(3.2)$ and a timestep $h = 1\mathrm{E}-2$, which for both methods resulted in solution trajectories with three impacts. In each respective figure we see the stable behavior of the truncated MH for each respective method. We also see significant dynamics in each of H and $-D_3L_d$, the energy functions underlying the respective reset maps for CVA and VCI. As mentioned prior, given that H and $-D_3L_d$ vary during portions of smooth integration, it seems a poor choice for CVA and VCI to enforce conservation of these quantities at impact.

Having observed the energy stability provided by MCVAA and MCVAC, now let us examine the accuracy of these methods with regards to trajectory errors. A plot of the L^2 error associated with the simulations for 51 distinct samples of the initial condition parameter β is presented in Figure 4. Errors are computed relative to a benchmark simulation which used a timestep $h = 10E-4$ and the CVA scheme.[§§§] Immediately we see that the MCVAA method, the only one out of the four methods that is based in SVA, provides the smallest errors. For the majority of initial conditions, CVA, VCI, and MCVAC offer comparable accuracy. That MCVAC is clustered with CVA and VCI, and not MCVAA, indicates that a simulation's energy stability does not formally guarantee greater simulation accuracy. Also of note is the jagged behavior in the results for VCI (especially at larger time steps). Further investigation revealed that this behavior correlates with unevenness in partial timestepping as β is varied. That is, jaggedness is associated with instances in which two successive samples of β yield simulations with significantly different (short vs. long) partial timesteps prior to impact events.

We also examined the computational effort of the MH-based methods, MCVAA and MCVAC. Results regarding average computation time, over 51 simulations in the aforementioned initial

[§§§] Additional simulations were performed to verify that the benchmark timestep was small enough such that the choice of integrator and impact map did not significantly impact results.

DOI: 10.1002/nme

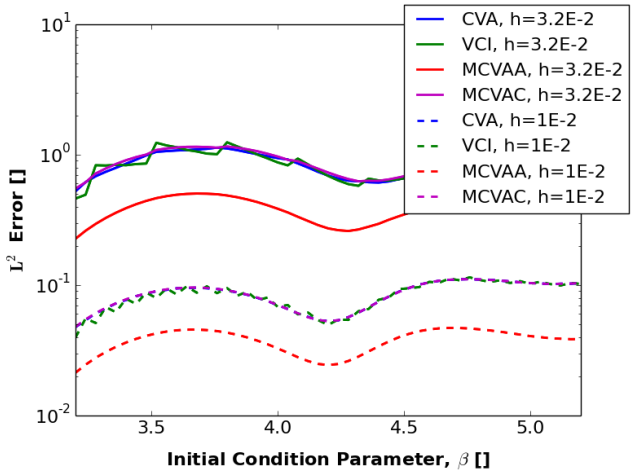

Figure 4. The L^2 trajectory error of simulations of the vertical cart-pendulum with impacts as a function of the initial condition parameter β. Across the spectrum of initial conditions MCVAA provides greater accuracy than the three competing methods, CVA, VCI, and MCVAC. Simulations use a final time of 5 seconds and a constant timestep of either $h = 3.2\text{E}-2$ or $h = 1\text{E}-2$.

Table II. Computation times, provided as 95% confidence intervals, of the MCVAA and MCVAC methods for simulations of 5 seconds of the cart-pendulum with impacts. Statistics were collected from 51 simulations of each method, using either $h = 3.2\text{E}-2$ or $h = 1\text{E}-2$. For the presented range of timesteps h, MCVAA, which uses a more costly method for smooth integration, outperforms MCVAC, which uses a more costly impact map. Naturally, this relationship between methods is dependent on the sparsity of collisions in the system dynamics.

Method	Computation Time [sec.]	
	$h = 3.2E-1$	$h = 1E-2$
MCVAA	2.71 ± 0.61	2.40 ± 0.39
MCVAC	1.55 ± 0.33	1.85 ± 0.22

condition space, are presented in Table II. We found that, in our selected range of timesteps, cart-pendulum simulations using MCVAA required less time than MCVAC. In terms of computational effort, the impact map associated with MCVAC requires more implicit solves than that of MCVAA. However, in using the SVA integrator on a nonseparable system, the MCVAA method requires twice as many implicit solves[¶¶¶] as MCVAC during portions of smooth integration. Hence MCVAC is the method better suited to systems exhibiting, over time, sparse collisions. In our sample simulations of the cart-pendulum, the collisions were dense enough to provide MCVAA the advantage.

It is also worth mentioning, in our selected range of timesteps the computation time of MCVAC decreases as timestep decreases. Though the effort used for smooth integration increases with decreasing timestep, the effort expended executing the impact map decreases due to improved initialization and conditioning. For these relatively large timesteps, the total effort of MCVAC is dominated by computing the impact map and thus the simultaneous decrease of effort and timestep is possible. For some smaller range of timesteps, the effort required for smooth integration will outweigh that for the impact map and this result will not persist. This lack of monotonicity in accuracy versus computational effort is one reason we chose to compare methods at fixed timesteps, rather than fixed accuracy or fixed effort.

[¶¶¶]Each half step, one of SE1 and one of SE2, requires an implicit solve in this case.

DOI: 10.1002/nme

6. CONCLUSIONS

We have established an expression of the modified Hamiltonian, and thus its modified equations, in terms of the discrete Lagrangian for a given VI. This theoretical development enabled the generalization of the MCVA algorithm to nonseparable systems and any choice of variational integrator. The resulting family of impact integration methods provides solutions to nonsmooth Hamiltonian modified equations to a user-specified level of accuracy. In doing so, the methods also preserve an associated symplectic form to a user-specified level of accuracy. In the instance that an explicit discrete Lagrangian is chosen, the inclusion of external nonconservative forces is explicit according to the discrete Larange-d'Alembert principle. The prescribed impact integration methods are the first to admit all three of these aforementioned properties–Hamiltonian modified equations, symplecticity, and explicit generating functions–when simulating general nonseparable nonsmooth mechanical systems.

We have evaluated and compared the performance of collision integrators on nonseparable systems, performing a variety of simulations of a vertical cart-pendulum with impacts. Using samples from a one-parameter family of initial conditions, we found that according to their design both MCVAA and MCVAC provided stable evolution of their respective truncated MH. However, this energy stability translated into simulation accuracy only in the case of MCVAA. It appears that, for the example cart-pendulum system, the choice of smooth integration scheme has a greater influence than the choice of impact map on the accuracy of resulting trajectories.

When comparing the computation times of the MH-based methods MCVAA and MCVAC, we found that MCVAA required less time due to the density of the cart-pendulum's collisions and MCVAC's more costly reset map. For other systems (or in different operating regimes of the cart-pendulum) in which collisions are very sparse, MCVAC offers computational savings due to the relative inexpense during portions of smooth integration. Lastly, given our aforementioned discussion of the discrete Lagrange-d'Alembert principle, MCVAC is more readily adapted, than MCVAA, to applications involving external nonconservative forces.

A. PRACTICAL COMPUTATION OF MODIFIED HAMILTONIAN TRUNCATIONS USING THE DISCRETE LAGRANGIAN

For completeness, in the following we detail the computations necessary to produce the higher order terms H_i in the series expression of the modified Hamiltonian $\widetilde{H}$ in Theorem 2. As stated prior, these terms can be expressed as functions of the discrete Lagrangian and its derivatives. Assume we begin with knowledge of consecutive phases (q_{k-1}, p_{k-1}) and (q_k, p_k) during a VI simulation using Φ_h corresponding to some prescribed L_d. The steps to compute terms $H_i(q_k, p_k)$ in $\widetilde{H}$ are then:

1. Calculate $\bar{q}_{k+1}$ satisfying

$$p_k = D_2 L_d(q_k, \bar{q}_{k+1}, h).$$

This relationship first appeared as equation (22) which served to implicitly define the mixed variable generating function $\widehat{S}(q_0, p_1)$. Calculations regarding $\widetilde{H}$ involve applying the definition of $\widehat{S}$ at a single time node, and thus the implicit definition of $\bar{q}_{k+1}$ above results. Note that $\bar{q}_{k+1}$ is *not* the same as the q_{k+1} produced by $\Phi_h(q_k, p_k)$.

DOI: 10.1002/nme

2. Regarding $\bar{q}_{k+1}$ as a function $\bar{q}_{k+1}(q_k, p_k)$, calculate partial derivatives of $\bar{q}_{k+1}$. For an $O(h^4)$ truncation of $\widetilde{H}$, this requires computing

$$\begin{aligned}
D_1\bar{q}_{k+1}\cdot v_1 &= -(D_2D_2L_d)^{-1}D_1D_2L_d\cdot v_1,\\
D_2\bar{q}_{k+1}\cdot v_1 &= (D_2D_2L_d)^{-1}\cdot v_1,\\
D_1D_2\bar{q}_{k+1}\cdot(v_1,v_2) &= (D_2D_2L_d)^{-1}D_1D_2D_2L_d\cdot\left((D_2D_2L_d)^{-1}\cdot v_1, v_2\right)\\
&\quad + (D_2D_2L_d)^{-1}D_2D_2D_2L_d\cdot\left((D_2D_2L_d)^{-1}\cdot v_1, D_1\bar{q}_{k+1}\cdot v_2\right),\\
D_1D_1\bar{q}_{k+1}\cdot(v_1,v_2) &= -D_1D_2\bar{q}_{k+1}\cdot(D_1D_2L_d\cdot v_1, v_2)\\
&\quad - (D_2D_2L_d)^{-1}D_1D_1D_2L_d\cdot(v_1,v_2)\\
&\quad - (D_2D_2L_d)^{-1}D_2D_1D_2L_d\cdot(v_1, D_1\bar{q}_{k+1}\cdot v_2),\\
D_2D_2\bar{q}_{k+1}\cdot(v_1,v_2) &= (D_2D_2L_d)^{-1}D_2D_2D_2L_d\cdot\left((D_2D_2L_d)^{-1}\cdot v_1, D_2\bar{q}_{k+1}\cdot v_2\right),
\end{aligned}$$

where all instances of L_d are evaluated at $(q_k, \bar{q}_{k+1}, h)$.

3. Calculate $\eta(q_k, p_k)$ according to equation (24), in which $\bar{q}_{k+1}$ appears as

$$\eta(q_k,p_k) = p_k\cdot\frac{\bar{q}_{k+1}-q_k}{h} - \frac{1}{h}L_d(q_k,\bar{q}_{k+1},h).$$

Also calculate higher order derivatives of $\eta(q_k, p_k)$. The first several of these take the form

$$\begin{aligned}
D_1\eta\cdot v_1 &= -\frac{p_k + D_1L_d}{h}\cdot v_1,\\
D_2\eta\cdot v_1 &= \frac{\bar{q}_{k+1}-q_k}{h}\cdot v_1,\\
D_1D_1\eta\cdot(v_1,v_2) &= -\frac{1}{h}D_1D_1L_d\cdot(v_1,v_2) - \frac{1}{h}D_2D_1L_d\cdot(v_1, D_1\bar{q}_{k+1}\cdot v_2),\\
D_1D_2\eta\cdot(v_1,v_2) &= \frac{1}{h}\left(D_1\bar{q}_{k+1} - \mathbb{I}\right)\cdot(v_1,v_2),\\
D_2D_2\eta\cdot(v_1,v_2) &= \frac{1}{h}D_2\bar{q}_{k+1}\cdot(v_1,v_2),
\end{aligned}$$

where $\mathbb{I}$ signifies the n-dimensional identity matrix acting as a bilinear operator, and all instances of L_d are evaluated at $(q_k, \bar{q}_{k+1}, h)$.

4. Expand the solution $\widetilde{S}(q,p,t)$ to the Hamilton-Jacobi PDE associated with the modified equations (recall the proof of Theorem 2) to the desired number of terms. For an $O(h^4)$ truncation of $\widetilde{H}$ we will need

$$\widetilde{S}(q,p,t) = t\widetilde{S}_1(q,p,h) + t^2\widetilde{S}_2(q,p,h) + t^3\widetilde{S}_3(q,p,h) + t^4\widetilde{S}_4(q,p,h) + \ldots,$$

where the terms $\widetilde{S}_i(q,p,h)$ are as determined in equation (30). We restate them here, but using compact slot derivative notation, as

$$\begin{aligned}
\widetilde{S}_1 &= \widetilde{H},\\
2\widetilde{S}_2 &= D_1\widetilde{H}\cdot D_2\widetilde{S}_1,\\
3\widetilde{S}_3 &= D_1\widetilde{H}\cdot D_2\widetilde{S}_2 + \frac{1}{2}D_1D_1\widetilde{H}\cdot\left(D_2\widetilde{S}_1, D_2\widetilde{S}_1\right),\\
4\widetilde{S}_4 &= D_1\widetilde{H}\cdot D_2\widetilde{S}_3 + D_1D_1\widetilde{H}\cdot\left(D_2\widetilde{S}_1, D_2\widetilde{S}_2\right) + \frac{1}{6}D_1D_1D_1\widetilde{H}\cdot\left(D_2\widetilde{S}_1, D_2\widetilde{S}_1, D_2\widetilde{S}_1\right).
\end{aligned}$$

In an attempt to maintain clarity in the application of higher order slot derivatives, we have included the vector arguments that contract with higher order derivatives of $\bar{q}_{k+1}$ when they are treated as tensors.

DOI: 10.1002/nme

Recalling the expansions

$$\widetilde{H} = \eta + hH_2 + h^2H_3 + h^3H_4 + \ldots,$$
$$\widetilde{S}_j = \widetilde{S}_{j1} + h\widetilde{S}_{j2} + h^2\widetilde{S}_{j3} + h^3\widetilde{S}_{j4} + \ldots,$$

and inserting them into the system of equations for $\widetilde{S}_i$ above, we have

$$\begin{aligned}
&\widetilde{S}_{11} + h\widetilde{S}_{12} + h^2\widetilde{S}_{13} + h^3\widetilde{S}_{14} + \ldots \\
&\qquad = \eta + hH_2 + h^2H_3 + h^3H_4 + \ldots, \\
&\widetilde{S}_{21} + h\widetilde{S}_{22} + h^2\widetilde{S}_{23} + \ldots \\
&\qquad = \frac{1}{2}\left(D_1\eta + hD_1H_2 + h^2D_1H_3 + \ldots\right)\cdot\left(D_2\widetilde{S}_{11} + hD_2\widetilde{S}_{12} + h^2D_2\widetilde{S}_{13} + \ldots\right), \\
&\widetilde{S}_{31} + h\widetilde{S}_{32} + \ldots \\
&\qquad = \frac{1}{3}\left(D_1\eta + hD_1H_2 + \ldots\right)\cdot\left(D_2\widetilde{S}_{21} + hD_2\widetilde{S}_{22} + \ldots\right) \\
&\qquad\quad + \frac{1}{6}\left(D_1D_1\eta + hD_1D_1H_2 + \ldots\right)\cdot\left(D_2\widetilde{S}_{11} + hD_2\widetilde{S}_{12} + \ldots, D_2\widetilde{S}_{11} + hD_2\widetilde{S}_{12} + \ldots\right), \\
&\widetilde{S}_{41} \\
&\qquad = \frac{1}{4}\left(D_1\eta + \ldots\right)\cdot\left(D_2\widetilde{S}_{31} + \ldots\right) \\
&\qquad\quad + \frac{1}{4}\left(D_1D_1\eta + \ldots\right)\cdot\left(D_2\widetilde{S}_{11} + \ldots, D_2\widetilde{S}_{21} + \ldots\right) \\
&\qquad\quad + \frac{1}{24}\left(D_1D_1D_1\eta + \ldots\right)\cdot\left(D_2\widetilde{S}_{11} + \ldots, D_2\widetilde{S}_{11} + \ldots, D_2\widetilde{S}_{11} + \ldots\right).
\end{aligned}$$

5. Use the relation $\widetilde{S}(q,p,h) = h\eta(q,p)$ to solve for all $\widetilde{S}_{jk}$ and H_i in terms of η and its derivatives. For the expansion above we obtain the expressions

$$\begin{aligned}
\widetilde{S}_{11} &= \eta, \\
\widetilde{S}_{21} &= \frac{1}{2}D_1\eta\cdot D_2\eta, \\
H_2 = \widetilde{S}_{12} &= -\widetilde{S}_{21}, \\
&= -\frac{1}{2}D_1\eta\cdot D_2\eta, \\
\widetilde{S}_{22} &= \frac{1}{2}D_1H_2\cdot D_2\widetilde{S}_{11} + \frac{1}{2}D_1\eta\cdot D_2\widetilde{S}_{12}, \\
&= -\frac{1}{4}D_1D_1\eta\cdot(D_2\eta, D_2\eta) - \frac{1}{2}D_1D_2\eta\cdot(D_1\eta, D_2\eta) - \frac{1}{4}D_2D_2\eta\cdot(D_1\eta, D_1\eta), \\
\widetilde{S}_{31} &= \frac{1}{3}D_1\eta\cdot D_2\widetilde{S}_{21} + \frac{1}{6}D_1D_1\eta\cdot\left(D_2\widetilde{S}_{11}, D_2\widetilde{S}_{11}\right), \\
&= \frac{1}{6}D_1D_2\eta\cdot(D_1\eta, D_2\eta) + \frac{1}{6}D_2D_2\eta\cdot(D_1\eta, D_1\eta) + \frac{1}{6}D_1D_1\eta\cdot(D_2\eta, D_2\eta),
\end{aligned}$$

DOI: 10.1002/nme

$$
\begin{aligned}
H_3 = \widetilde{S}_{13} &= -\widetilde{S}_{22} - \widetilde{S}_{31}, \\
&= \frac{1}{12}\Big(D_1D_1\eta\cdot(D_2\eta,D_2\eta) + 4D_1D_2\eta\cdot(D_1\eta,D_2\eta) + D_2D_2\eta\cdot(D_1\eta,D_1\eta)\Big), \\
\widetilde{S}_{23} &= \frac{1}{2}D_1H_3\cdot D_2\widetilde{S}_{11} + \frac{1}{2}D_1H_2\cdot D_2\widetilde{S}_{12} + \frac{1}{2}D_1\eta\cdot D_2\widetilde{S}_{13}, \\
&= \frac{1}{24}D_1D_1D_1\eta\cdot(D_2\eta,D_2\eta,D_2\eta) + \frac{5}{24}D_1D_1D_2\eta\cdot(D_1\eta,D_2\eta,D_2\eta) \\
&\quad + \frac{5}{24}D_1D_2D_2\eta\cdot(D_1\eta,D_1\eta,D_2\eta) + \frac{1}{24}D_2D_2D_2\eta\cdot(D_1\eta,D_1\eta,D_1\eta) \\
&\quad + \frac{3}{8}D_1D_1\eta\cdot(D_2D_1\eta\cdot(D_2\eta,\cdot),D_2\eta) + \frac{7}{24}D_1D_1\eta\cdot(D_2D_2\eta\cdot(D_1\eta,\cdot),D_2\eta) \\
&\quad + \frac{11}{24}D_1D_2\eta\cdot(D_1D_2\eta\cdot(D_1\eta,\cdot),D_2\eta) + \frac{3}{8}D_2D_2\eta\cdot(D_1D_2\eta\cdot(D_1\eta,\cdot),D_1\eta), \\
\widetilde{S}_{32} &= \frac{1}{3}D_1H_2\cdot D_2\widetilde{S}_{21} + \frac{1}{3}D_1\eta\cdot D_2\widetilde{S}_{22} \\
&\quad + \frac{1}{6}D_1D_1H_2\cdot\Big(D_2\widetilde{S}_{11},D_2\widetilde{S}_{11}\Big) + \frac{1}{3}D_1D_1\eta\cdot\Big(D_2\widetilde{S}_{11},D_2\widetilde{S}_{12}\Big), \\
&= -\frac{1}{12}D_1D_1D_1\eta\cdot(D_2\eta,D_2\eta,D_2\eta) - \frac{1}{6}D_1D_1D_2\eta\cdot(D_1\eta,D_2\eta,D_2\eta) \\
&\quad - \frac{1}{6}D_1D_2D_2\eta\cdot(D_1\eta,D_1\eta,D_2\eta) - \frac{1}{12}D_2D_2D_2\eta\cdot(D_1\eta,D_1\eta,D_1\eta) \\
&\quad - \frac{5}{12}D_1D_1\eta\cdot(D_2D_1\eta\cdot(D_2\eta,\cdot),D_2\eta) - \frac{5}{12}D_1D_1\eta\cdot(D_2D_2\eta\cdot(D_1\eta,\cdot),D_2\eta) \\
&\quad - \frac{1}{4}D_1D_2\eta\cdot(D_1D_2\eta\cdot(D_1\eta,\cdot),D_2\eta) - \frac{5}{12}D_2D_2\eta\cdot(D_1D_2\eta\cdot(D_1\eta,\cdot),D_1\eta), \\
\widetilde{S}_{41} &= \frac{1}{4}D_1\eta\cdot D_2\widetilde{S}_{31} + \frac{1}{4}D_1D_1\eta\cdot\Big(D_2\widetilde{S}_{11},D_2\widetilde{S}_{21}\Big) + \frac{1}{24}D_1D_1D_1\eta\cdot\Big(D_2\widetilde{S}_{11},D_2\widetilde{S}_{11},D_2\widetilde{S}_{11}\Big), \\
&= \frac{1}{24}D_1D_1D_1\eta\cdot(D_2\eta,D_2\eta,D_2\eta) + \frac{1}{24}D_1D_1D_2\eta\cdot(D_1\eta,D_2\eta,D_2\eta) \\
&\quad + \frac{1}{24}D_1D_2D_2\eta\cdot(D_1\eta,D_1\eta,D_2\eta) + \frac{1}{24}D_2D_2D_2\eta\cdot(D_1\eta,D_1\eta,D_1\eta) \\
&\quad + \frac{1}{8}D_1D_1\eta\cdot(D_2D_1\eta\cdot(D_2\eta,\cdot),D_2\eta) + \frac{5}{24}D_1D_1\eta\cdot(D_2D_2\eta\cdot(D_1\eta,\cdot),D_2\eta) \\
&\quad + \frac{1}{24}D_1D_2\eta\cdot(D_1D_2\eta\cdot(D_1\eta,\cdot),D_2\eta) + \frac{1}{8}D_2D_2\eta\cdot(D_1D_2\eta\cdot(D_1\eta,\cdot),D_1\eta), \\
H_4 = \widetilde{S}_{14} &= -\widetilde{S}_{23} - \widetilde{S}_{32} - \widetilde{S}_{41}, \\
&= -\frac{1}{12}\Big(D_1D_1D_2\eta\cdot(D_1\eta,D_2\eta,D_2\eta) + D_1D_2D_2\eta\cdot(D_1\eta,D_1\eta,D_2\eta) \\
&\quad + D_1D_1\eta\cdot(D_2D_1\eta\cdot(D_2\eta,\cdot),D_2\eta) + D_1D_1\eta\cdot(D_2D_2\eta\cdot(D_1\eta,\cdot),D_2\eta) \\
&\quad + 3D_1D_2\eta\cdot(D_1D_2\eta\cdot(D_1\eta,\cdot),D_2\eta) + D_2D_2\eta\cdot(D_1D_2\eta\cdot(D_1\eta,\cdot),D_1\eta)\Big).
\end{aligned}
$$

Computing the above expressions for H_i using the previously determined derivatives of η provides the terms needed for the $O(h^4)$ truncation of $\widetilde{H}(q_k,p_k)$:

$$\widetilde{H}^{O(h^4)}(q,p) = \eta(q,p) + hH_2(q,p) + h^2H_3(q,p) + h^3H_4(q,p).$$

For one familiar with backwards error analysis, the expressions for H_i above may appear familiar. They are precisely the terms in the series expansion of $\widetilde{H}$ for symplectic Euler 1, but with η appearing in place of H. This follows from the fact that the definition of $\eta(q_0,p_1)$ in equation (24), when using the SE1 discrete Lagrangian L_d^{SE1}, simplifies to $H(q_0,p_1)$. In other words, the

DOI: 10.1002/nme

mixed variable generating function for SE1 is

$$\widehat{S}^{\mathrm{SE1}}(q_0, p_1) = p_1 \cdot q_0 + hH(q_0, p_1),$$

which has the form of the generating function for general VIs, but with H in place of η.

REFERENCES

1. Pfeiffer F, Glocker C. *Multibody dynamics with unilateral contacts*. John Wiley & Sons: New York, 1996.
2. Chatterjee A, Ruina A. A new algebraic rigid-body collision law based on impulse space considerations. *Journal of Applied Mechanics-Transactions of the ASME* 1998; **65**(4):939–951.
3. Terzopoulos D, Platt J, Barr A, Fleischer K. Elastically deformable models. *SIGGRAPH Comput. Graph.* Aug 1987; **21**(4):205–214, doi:10.1145/37402.37427.
4. Harmon D, Vouga E, Smith B, Tamstorf R, Grinspun E. Asynchronous contact mechanics. *ACM SIGGRAPH*, ACM: New York, NY, USA, 2009; 87:1–87:12, doi:10.1145/1576246.1531393.
5. Marques MDPM. *Differential inclusions in nonsmooth mechanical problems: Shocks and dry friction*, vol. 9. Birkhauser, 1993.
6. Mabrouk M. A unified variational model for the dynamics of perfect unilateral constraints. *European Journal of Mechanics - A/Solids* 1998; **17**(5):819 – 842, doi:10.1016/S0997-7538(98)80007-7.
7. Brogliato B. *Nonsmooth mechanics: models, dynamics, and control*. Communications and control engineering series, Springer, 1999.
8. Glocker C. *Set-valued force laws: dynamics of non-smooth systems*, *Lecture Notes in Applied Mechanics*, vol. 1. Springer, 2001.
9. Brogliato B. Some perspectives on the analysis and control of complementarity systems. *IEEE Transactions on Automatic Control* 2003; **48**(6):918–935.
10. Heemels WPMH, Schumacher JM, Weiland S. Linear complementarity systems. *SIAM Journal on Applied Mathematics* 2000; :1234–1269.
11. Glocker C. The principles of d'Alembert, Jourdain, and Gauss in nonsmooth dynamics. Part I: Scleronomic multibody systems. *ZAMM* 1998; **78**(1):21–37.
12. Leine RI, Aeberhard U, Glocker C. Hamilton's principle as variational inequality for mechanical systems with impact. *Journal of Nonlinear Science* 2009; **19**(6):633–664.
13. Kozlov VV, Treshchëv DV. *Billiards: a genetic introduction to the dynamics of systems with impacts*. Translations of mathematical monographs, American Mathematical Society, 1991.
14. Fetecau RC, Marsden JE, Ortiz M, West M. Nonsmooth Lagrangian mechanics and variational collision integrators. *SIAM Journal on Applied Dynamical Systems* 2003; **2**:381–416, doi:10.1137/S1111111102406038.
15. Acary V, Brogliato B. *Numerical methods for nonsmooth dynamical systems: applications in mechanics and electronics*, *Lecture Notes in Applied and Computational Mechanics*, vol. 35. Springer-Verlag, 2008.
16. Stewart DE, Trinkle JC. An implicit time-stepping scheme for rigid body dynamics with Coulomb friction. *International Journal for Numerical Methods in Engineering* 1996; **39**(15):2673–2691.
17. Moreau JJ. Numerical aspects of the sweeping process. *Computer methods in applied mechanics and engineering* 1999; **177**(3):329–349.
18. Paoli L, Schatzman M. A numerical scheme for impact problems I: The one-dimensional case. *SIAM Journal on Numerical Analysis* 2002; **40**(2):702–733.
19. Paoli L, Schatzman M. A numerical scheme for impact problems II: The multidimensional case. *SIAM journal on numerical analysis* 2002; **40**(2):734–768.
20. Studer C. *Numerics of unilateral contacts and friction: modeling and numerical time integration in non-smooth dynamics*, *Lecture Notes in Applied and Computational Mechanics*, vol. 47. Springer-Verlag, 2009.
21. Kaufman D, Pai D. Geometric numerical integration of inequality constrained, nonsmooth Hamiltonian systems. *SIAM Journal on Scientific Computing* 2012; **34**(5):A2670–A2703, doi:10.1137/100800105.
22. Houndonougbo YA, Laird BB, Leimkuhler BJ. A molecular dynamics algorithm for mixed hard-core/continuous potentials. *Molecular Physics* 2000; **98**(5):309–316, doi:10.1080/00268970009483294.
23. Janin O, Lamarque CH. Comparison of several numerical methods for mechanical systems with impacts. *International Journal for Numerical Methods in Engineering* 2001; **51**(9):1101–1132.
24. Bond SD, Leimkuhler BJ. Stabilized integration of Hamiltonian systems with hard-sphere inequality constraints. *SIAM J. Sci. Comput.* November 2007; **30**:134–147, doi:10.1137/06066552X.
25. Marsden JE, West M. Discrete mechanics and variational integrators. *Acta Numerica* 2001; **10**:357–514.
26. Hairer E, Lubich C, Wanner G. *Geometric numerical integration: structure-preserving algorithms for ordinary differential equations*, *Springer Series in Computational Mathematics*, vol. 31. Second edn., Springer-Verlag: Berlin, 2006.
27. Leyendecker S, Marsden J, Ortiz M. Variational integrators for constrained mechanical systems. *ZAMM* 2008; **88**:677–708.
28. McLachlan R, Perlmutter M. Integrators for nonholonomic mechanical systems. *J. Nonlinear Sci.* 2006; **16**(4):283–328.
29. Bou-Rabee N, Marsden JE. Hamilton–Pontryagin integrators on lie groups part i: Introduction and structure-preserving properties. *Foundations of Computational Mathematics* 2009; **9**:197–219. 10.1007/s10208-008-9030-4.
30. Benettin G, Giorgilli A. On the Hamiltonian interpolation of near to the identity symplectic mappings with application to symplectic integration algorithms. *J. Stat. Phys* 1994; **74**:1117–1143.
31. Goldstein H, Poole CP, Safko JL. *Classical Mechanics*. 3rd edition edn., Addison Wesley, 2001.

32. Ohsawa T, Bloch A, Leok M. Discrete Hamilton–Jacobi theory and discrete optimal control. *Proc. IEEE Conf. on Decision and Control* 2010; :5438–5443doi:10.1109/CDC.2010.5717665.
33. Marsden JE, Ratiu TS. *Introduction to Mechanics and Symmetry*, *Texts in Applied Mathematics*, vol. 17. Springer-Verlag: New York, 1999.
34. Hairer E, NøRsett SP, Wanner G. Geometric numerical integration illustrated by the störmer-verlet method. *Acta Numerica* 2003; **12**:399–450, doi:10.1017/S0962492902000144.
35. Lall S, West M. Discrete variational Hamiltonian mechanics. *J. Phys. A* 2006; **39**(19):5509–5519.
36. Mackay R. Some aspects of the dynamics of Hamiltonian systems. *The Dynamics of numerics and the numerics of dynamics*, Broomhead DS, Iserles A (eds.). Clarendon Press: Oxford, 1992; 137–193.
37. Kane C, Marsden JE, Ortiz M, West M. Variational integrators and the newmark algorithm for conservative and dissipative mechanical systems. *Int. J. Num. Math. Eng.* 2000; **49**:1295–1325.